Electrochimica Acta 54 (2008) 524–529

Contents lists available at ScienceDirect

Electrochimica Acta

journal homepage: www.elsevier.com/locate/electacta

Electrodeposition of $CuInSe_2$ and In_2Se_3 on flat and nanoporous TiO_2 substrates

M. Valdés[a,b], M. Vázquez[a,*,1], A. Goossens[b]

[a] División Corrosión, INTEMA, Facultad de Ingeniería, Universidad Nacional de Mar del Plata Juan B. Justo 4302 – B7608FDQ Mar del Plata, Argentina
[b] Optoelectronic Materials, Faculty of Applied Sciences, Delft University of Technology, Julianalaan 136, 2628 BL Delft, The Netherlands

ARTICLE INFO

Article history:
Received 27 May 2008
Received in revised form 10 July 2008
Accepted 13 July 2008
Available online 23 July 2008

Keywords:
Electrodeposition
TiO_2
$CuInSe_2$
Buffer layer
Heterojunction

ABSTRACT

In_2Se_3 and $CuInSe_2$ films have been prepared by potentiostatic electrodeposition from deareated aqueous solutions. The substrate consisted of a duplex layer of dense and nanoporous TiO_2 obtained by spray pyrolysis deposition (SPD) and doctor blading. In_2Se_3 thin films are electrodeposited in between the TiO_2/$CuInSe_2$ pn heterojunction to block the electron back flow and lower the interfacial recombination produced upon illumination. The films have been characterized using X-ray diffraction, Raman spectroscopy, scanning electron microscopy, and optical transmission. Annealing the samples in Se atmosphere is essential to improve the crystallinity of the In_2Se_3 and $CuInSe_2$ films. The combination of TiO_2/In_2Se_3/$CuInSe_2$ shows very good diode behavior with a rectification ratio higher than 100 at ±1 V.

1. Introduction

One of the main obstacles for photovoltaics to compete on the energy market is the price of electricity (cost per watt) produced in a solar cell, which is considerable higher than that produced by conventional methods. Cost reduction can be achieved by either improving the efficiency or by reducing the production costs of photovoltaic modules.

In order to reduce production costs, new cell concepts based on nanostructured materials have been developed. Grätzel and O'Regan introduced an important advancement by using nanostructured titanium dioxide in dye-sensitized solar cells [1]. Other groups have used a similar concept to design new cells based on 3D inorganic heterojunctions, achieving conversion efficiencies of 5% by atomic layer deposition (ALD) and spray pyrolysis deposition (SPD) [2]. In our opinion, significant cost reduction can only be accomplished when batch-wise production, including vacuum or controlled gas conditions, is avoided. Both spray deposition and electrodeposition can be applied in an industrial bulk production process and are therefore the deposition methods of choice.

Chalcopyrites, particularly $CuInSe_2$ (copper indium diselenide, CISe), are among the most promising absorbing materials for solar cells. CISe-based solar cells are very stable, allowing long operational lifetimes. The favorable optical properties of these materials (direct band gap and high absorption coefficient) enable the use of thin films (few micrometers) instead of thick slices of bulk silicon, reducing the consumption of expensive materials. CISe-based thin films can be prepared both from gas and liquid phases by a variety of methods.

Electrodeposition is a liquid phase method that can be used for the preparation of metal, semiconductor, and conducting oxide thin films. Its advantages include the feasibility of upscaling to large substrate areas and production volumes. Moreover, the deposition equipment is relatively simple and the deposition temperatures are considerably lower than in many other methods. These features make electrodeposition an attractive, low-cost deposition method.

High conversion efficiencies have been achieved in solar cells that incorporate electrodeposited CISe [3]. In these studies, however, Mo-coated glass is used as substrate. Sputter deposition is used to obtain the substrate, which boosts the production costs of these cells.

Our previous work [4] shows that the electrodeposition of $CuInSe_2$ inside a nanoporous matrix of TiO_2 is possible. However, the conversion of sunlight into electricity is very low. In this work, the incorporation of In_2Se_3 acting as a, so-called, buffer layer is tested in an attempt to improve the conversion efficiency. Conversion enhancement can be achieved by blocking the electron back flow and by lowering the interfacial recombination. The present investigations focus on revealing the parameters that govern the electrodeposition of In_2Se_3 on TiO_2 and of CISe onto In_2Se_3.

* Corresponding author. Tel.: +54 223 481 6600; fax: +54 223 481 0046.
E-mail address: mvazquez@fi.mdp.edu.ar (M. Vázquez).
[1] ISE active member.

0013-4686/$ – see front matter © 2008 Elsevier Ltd. All rights reserved.
doi:10.1016/j.electacta.2008.07.036

2. Experimental aspects

Glass coated with a transparent conducting tin oxide (TCO, SnO_2:F, Libbey Owens Ford, TEC 8/3 mm) is used as substrate. It is degreased in an ultrasonic bath with ethanol three times during 15 min prior to use.

On top of this, a dense-TiO_2 layer (d-TiO_2) is deposited by spray pyrolysis deposition (SPD). A precursor solution containing 2.4 ml titanium IV isopropoxide (TTIP) as a titanium source, 3.6 ml acetylacetone (AcAc) as a stabilizer and 54 ml ethanol as solvent is prepared. The solution is atomized by a pneumatic spray system using oxygen as the gas carrier. The films are deposited using a pulsed solution feed at a substrate temperature of 350 °C. The pulse consisted of 1 min of continuous spray and 1 min of delay. The resulting layer prevents direct contact between the highly doped SnO:F (TCO) and the electrodeposited In_2Se_3 or $CuInSe_2$ avoiding short circuiting of the cell. Next, a nanocrystalline-TiO_2 coating (nc-TiO_2) is applied by doctor blading [5], using particles of 25 nm of average diameter. In doctor blade deposition, a sol (viscous paste) is prepared using commercial TiO_2 (P25, Degussa AG, Germany). In order to break the aggregates into separate particles, the powder (6 g) is ground in a porcelain mortar with a small amount of water (2 ml) containing acetylacetone (0.2 ml) to prevent reaggregation of the particles. After the powder has been dispersed by the high shear forces in the viscous paste, it is diluted by slow addition of water (8 ml) under continuous grinding. Finally, a detergent (0.1 μl Triton X-100) is added to facilitate the spreading of the colloid on the substrate. The conducting TCO glass is covered on two parallel edges with adhesive tape to control the thickness of the TiO_2 film. The colloid is applied to one of the free edges of the substrate and distributed with a glass rod sliding over the tape-covered edges. After air drying, the sample is treated for 6 h at 450 °C in air. This sintering process is necessary to obtain a highly crystalline electron-conducting matrix. The resulting film thickness is 2 μm but can be varied by changing the colloid concentration or the adhesive tape thickness.

Following the duplex TiO_2 layer, a thin film of In_2Se_3 is electrodeposited potentiostatically, as described in the work of Massaccesi et al. [6]. A precursor solution of 2 mM $InCl_3$, 1 mM SeO_2 is used with the addition of 0.3 M KCl as supporting electrolyte. The pH is adjusted to 2.5 using concentrated HCl. The process is carried out at 80 °C in a stirred solution purged with nitrogen. A three-electrode configuration is used, with a saturated calomel electrode used as reference (SCE = +0.24 V vs. SHE) and a Pt mesh of large area as counter electrode. In_2Se_3 films were deposited at −0.7 and −0.8 V (vs. SCE) during different times (between 5 and 20 min) in order to achieve a variety of film thicknesses.

Finally, on top of the In_2Se_3 layer, a thin film of $CuInSe_2$ (CISe) is electrodeposited. The precursor solution contains 1 mM $CuCl_2$, 3 mM $InCl_3$ and 1.7 mM SeO_2 with a pH of 2. The electrodeposition was carried out at −0.8 V during different periods of time (between 5 and 60 min). Most of the results are presented for films deposited during 60 min. More experimental details of the electrodeposition of CISe can be found in our previous work [4].

All the electrochemical measurements were carried out using a Princeton Applied Research Potentiostat/Galvanostat model 273.

The thickness of the electrodeposited films (T) can be calculated using Eq. (1), based on Faraday's law

$$T = \frac{1}{nFA}\left(\frac{itM}{\rho}\right) \quad (1)$$

where n is the number of electrons transferred, F is Faraday's number, A is the electrode area, i is the current, t is the deposition time, M is the formula weight, and ρ is the density.

In electrodepositing In_2Se_3, the number of electrons transferred is 18 according to the total electrode reaction:

$$2In^{3+} + 3SeO_3{}^{2-} + 18H^+ + 18e^- \rightarrow In_2Se_3 + 9H_2O \quad (2)$$

The molar mass and density values used are M = 466.52 g/mol and ρ = 5.74 g/cm^3 [7].

In the case of CISe, 13 electrons are exchanged taking the following reaction into account:

$$Cu^{2+} + In^{3+} + 2SeO_3{}^{2-} + 12H^+ + 13e^- \rightarrow CuInSe_2 + 6H_2O \quad (3)$$

In this case, M = 336.28 g/mol and ρ = 5.77 g/cm^3 [8].

These are approximations, since the formula weights and densities vary with the composition and the efficiency of electrodeposition process is assumed to be 100%.

To improve the crystallinity and to adjust the chemical composition of the as-deposited CISe films, the samples are annealed in a selenium atmosphere using a home-built rapid thermal anneal reactor. It consists of a tubular quartz tube placed inside a ceramic oven with two independently controlled temperature zones. The selenium atmosphere is established by heating elemental selenium at 280 °C, while the substrate is annealed at 400 °C during 30 min.

The excess of Cu- and Se-rich phases is removed by etching the films in 0.5 M KCN aqueous solution for different periods of time (10 s to 5 min) as described in the literature [9].

The crystal structure of the samples is determined by X-ray diffraction (Bruker D8 Advanced Diffractometer) using Cu Kα radiation and Ni–Cu slits filter. The operation voltage and current used are 40 kV and 40 mA, respectively. The diffraction patterns are recorded from $2\theta = 10°$ to 70°. The crystallographic data for each phase are taken from the literature [10].

Raman spectra are obtained using a Spectra Physics Millenia Nd:YVO4 with a wavelength of 532 nm in the backscattering mode, a set of notch filters to remove the Raleigh scatterings and a 340 Spex monochromator equipped with an 1800 grooves/mm grating.

The absorption coefficient α and the bandgap energy are calculated from the transmission spectra registered using an UV/Vis/NIR Spectrophotometer (λ900, PerkinElmer) in the wavelength range 350–2000 nm at room temperature.

To investigate the electric response of the cells, current–voltage curves of a representative device such as SnO_2:F/TiO_2(100 nm)/nc-TiO_2/In_2Se_3/CISe/graphite are performed.

3. Results and discussion

Fig. 1 shows an illustration of the spray pyrolysis process carried out to form dense TiO_2 films on TCO substrates. An XRD pattern typical of these films is presented in Fig. 2. Due to the fact that the film is very thin (∼150 nm) the signals of the anatase peaks are small and the main peaks belong to the substrate (SnO_2:F). However, the anatase structure is present, indicating the good crystallinity of the sprayed TiO_2 films. The Raman spectra (Fig. 3) confirm this conclusion and show intense scattering of the anatase TiO_2 vibration modes. Similar results (not shown here) were found with the nc-TiO_2 thick films prepared by doctor blading [4].

In_2Se_3 is then electrodeposited potentiostatically on top of a duplex layer of dense and nanocrystalline TiO_2 supported on TCO (TCO/d-TiO_2/nc-TiO_2). To evaluate the effect of time and potential, films are prepared at −0.7 and −0.8 V during different periods of time. Average values for the film thickness are presented in Table 1.

Fig. 4 shows the diffraction pattern of electrodeposited In_2Se_3 (as-deposited). The main peaks of the β-In_2Se_3 structure are present. This result is in agreement with other diffraction patterns of electrodeposited In_2Se_3 reported in the literature [6,11]. A Raman

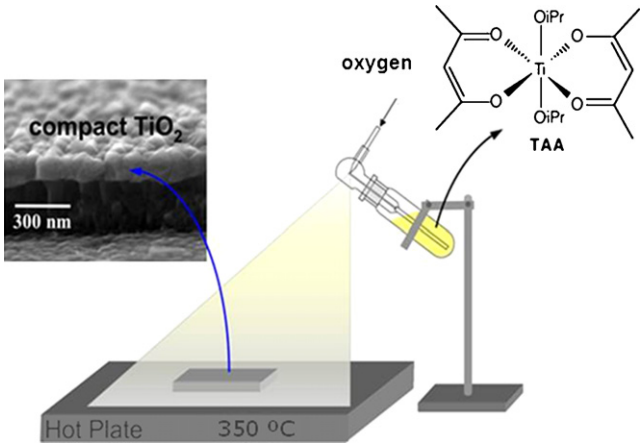

Fig. 1. Schematic picture of the spray pyrolysis process for the preparation of dense anatase TiO_2 films. The precursor solution contains titanium acetylacetonate (TAA) in ethanol and is atomized in pulses by a pneumatic spray system.

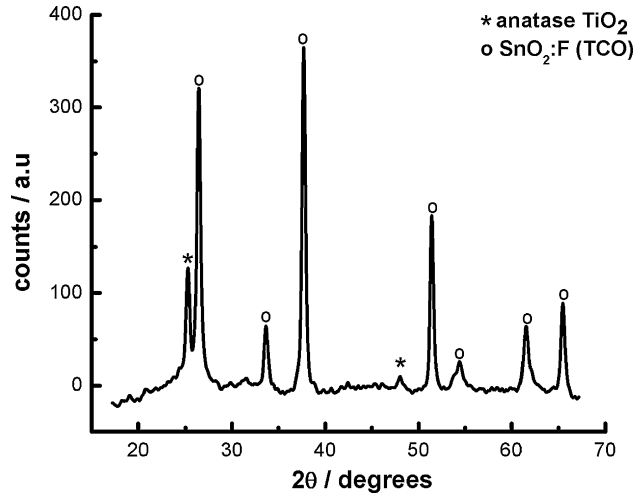

Fig. 2. XRD pattern of d-TiO_2, prepared by spray pyrolysis on a TCO substrate.

spectrum characteristic of electrodeposited In_2Se_3 films is shown in Fig. 5. Most of the signals belong to the anatase TiO_2 layers, but a broad peak at 253 cm^{-1} is distinctive of the In_2Se_3 phase. The strongest feature at 253 cm^{-1} and a shoulder at 235 cm^{-1} in the

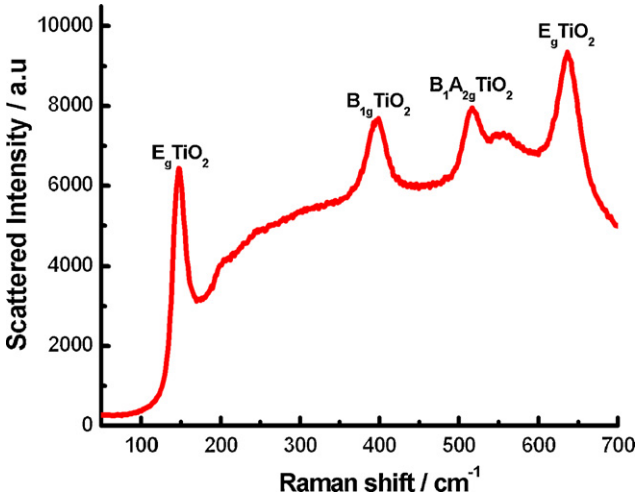

Fig. 3. Raman spectra of d-TiO_2, prepared by spray pyrolysis on a TCO substrate.

Table 1
Average thickness of as-deposited In_2Se_3 and $CuInSe_2$ films supported on TCO/d-TiO_2/nc-TiO_2, and obtained using various electrodeposition potentials and times

Time (min)	Film thickness (μm)		
	In_2Se_3		$CuInSe_2$
	−0.7 (V)	−0.8 (V)	−0.8 (V)
5	0.08	0.12	0.37
10	0.15	0.29	–
15		0.31	–
20	0.55	0.49	–
25	–	–	0.8
40	–	–	1.21
60	–	–	2.64

The calculations were carried out employing Eq. (1) and assuming 100% efficiency in each electrochemical process.

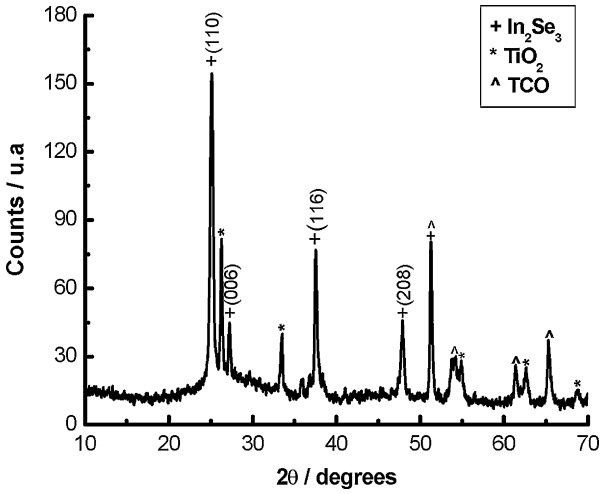

Fig. 4. XRD pattern of as-deposited In_2Se_3. The film is supported on TCO/d-TiO_2/nc-TiO_2 and prepared at 80 °C, holding the potential at −0.8 V (vs. SCE) during 20 min.

Raman spectrum of In_2Se_3 film are attributed to Se_8 rings and Se_n molecules [12].

SEM pictures of as-deposited In_2Se_3 and CISe are presented in Fig. 6. The films are homogenous and, in the case of In_2Se_3, formed

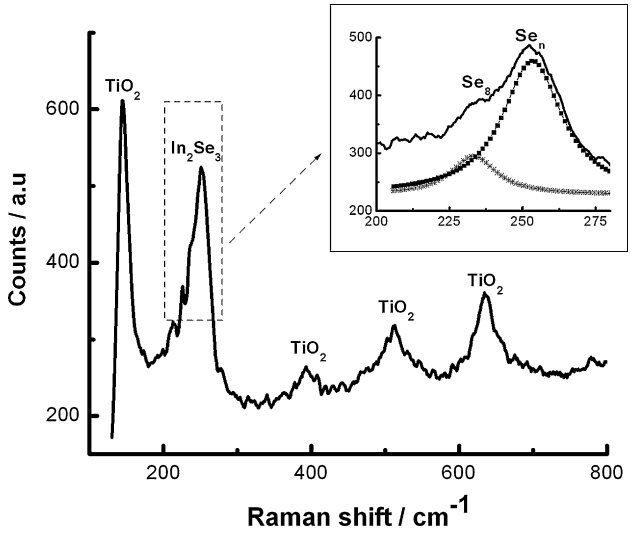

Fig. 5. Raman spectra of as-deposited In_2Se_3. The film is supported on TCO/d-TiO_2/nc-TiO_2, prepared at 80 °C, holding the potential at −0.8 V (vs. SCE) during 20 min. The inset shows the deconvoluted spectra of the In_2Se_3 peak.

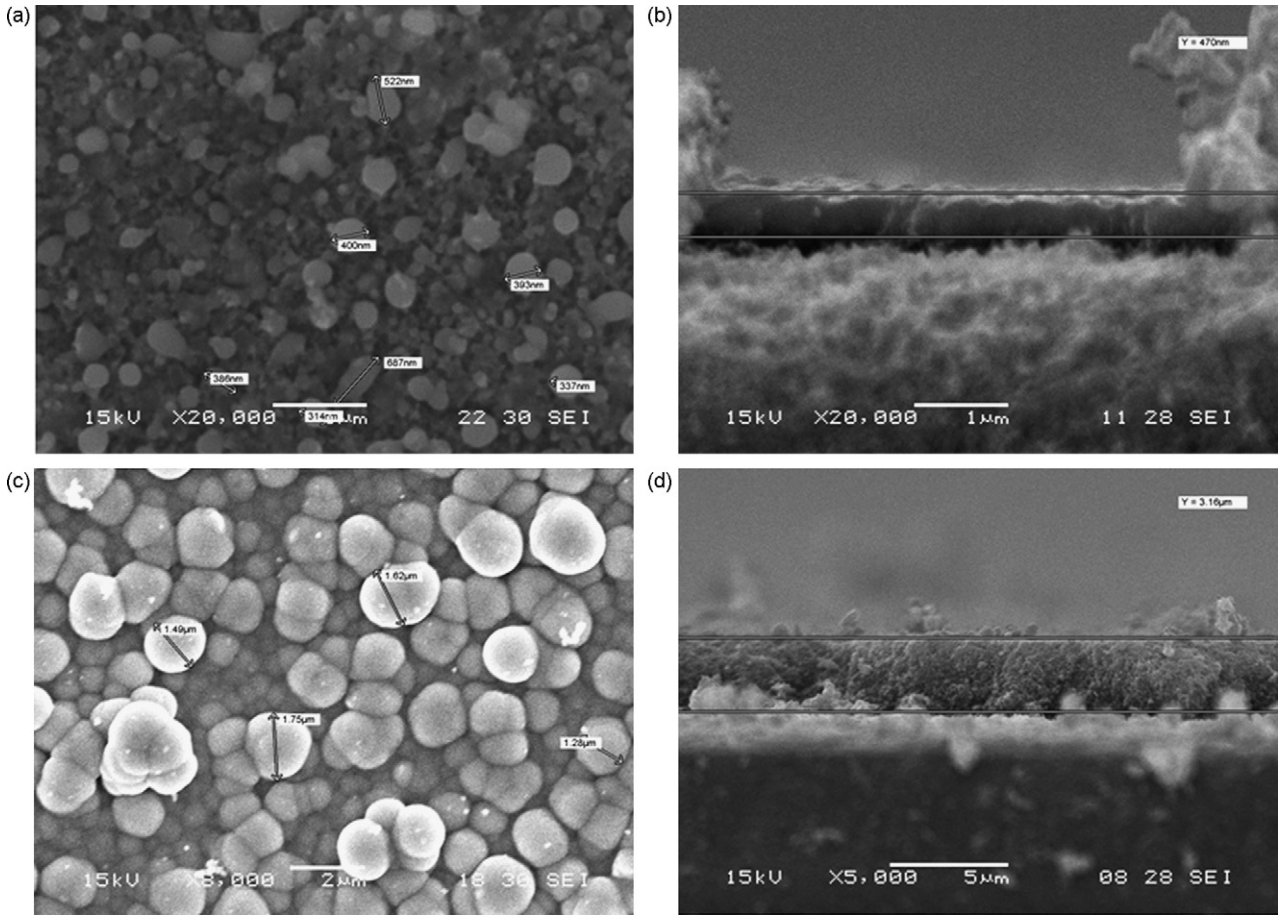

Fig. 6. SEM pictures of In_2Se_3 and CISe supported on TCO/d-TiO_2/nc-TiO2. In_2Se_3 is electrodeposited at −0.8 V during 20 min and CISe electrodeposited at −0.8 V during 60 min—(a) In_2Se_3: the frontal view shows a homogeneous film with particle size in the nanometer scale; (b) In_2Se_3: the cross-view shows an average thickness of 0.47 μm; (c) CISe: frontal view; and (d) CISe: the cross-view shows an average thickness of 3.16 μm.

by nanosized particles. Both films are supported on TCO/d-TiO_2/nc-TiO_2. A cross-section view of the deposits provides a more direct measurement for the thickness of the layers. Average values result in 0.47 μm for the thickness of In_2Se_3 deposited during 15 min a −0.8 V and 3.16 μm in the case of CISe deposited for 60 min. The values are in relatively good agreement with those presented in Table 1.

Fig. 7 shows XRD diffraction spectra before and after annealing in Se vapor. The improvement in the crystallinity of CISe films after a thermal treatment in Se atmosphere can be clearly seen. Furthermore, secondary phases are usually found in the film after annealing [13–17]. One of these secondary phases is also identified using Raman spectroscopy, as shown in Fig. 8. The spectrum of the annealed film contains the A_1 mode signal between 175 and 178 cm^{-1}, generally observed in $CuInSe_2$ and an additional peak at 258 cm^{-1}. This last peak is related to the presence of a Cu_xSe secondary phase [18,19]. In particular, this phase can severely damage the electronic properties of the CISe devices, so that it has to be removed from the film. Etching in concentrated KCN solution is a well-known method to achieve this goal, enabling a complete elimination of the undesired Cu_xSe phase. In addition, some of the CISe phase itself is removed. An indication of this is a small reduction in the intensity of the A_1 signal and the appearance of a TiO_2 signal that is not present in the non-etched sample, as reported elsewhere [4].

Furthermore Raman spectroscopy is powerful technique to investigate the deposition process of CISe on TiO_2 substrates. In Fig. 8, the spectra of as-deposited CISe films at different times indicate that at short times of electrodeposition (5 and 15 min) the film mainly consists of Cu_xSe as secondary phase while at longer times of deposition (45 and 60 min) the A_1 modes signal starts to grow indicating the presence of CISe in the film. This can be related to the reaction of In^{3+} ions with the $CuSe_x$ previously deposited to form

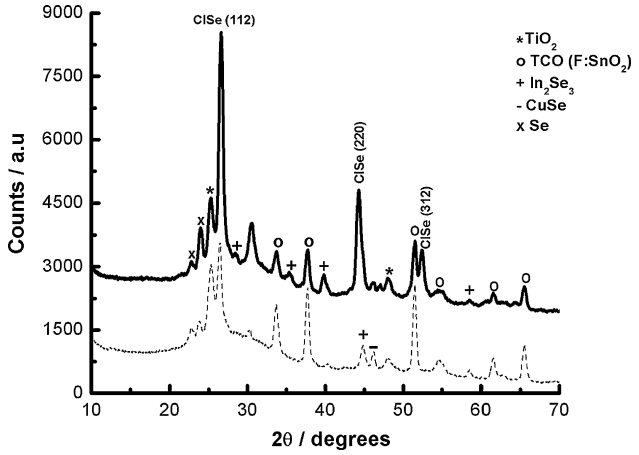

Fig. 7. XRD pattern of a TCO/d-TiO_2/nc-TiO_2/In_2Se_3/$CuInSe_2$ cell. The CISe film was electrodeposited at −0.8 V during 60 min (- - -) as-deposited, (—) annealed in Se at 400 °C for 30 min.

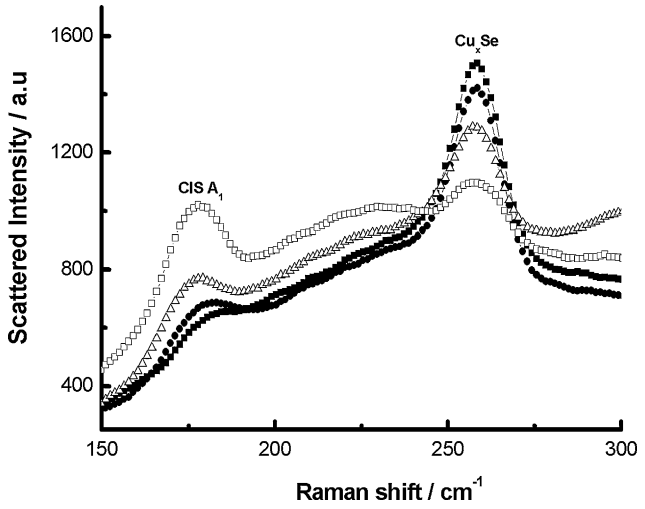

Fig. 8. The effect of the electrodeposition time in as-deposited CISe samples supported on TCO/d-TiO_2/nc-TiO_2/In_2Se_3. $E = -0.8$ V (vs. SCE). (■) 5 min; (●) 15 min; (△) 40 min and (□) 60 min.

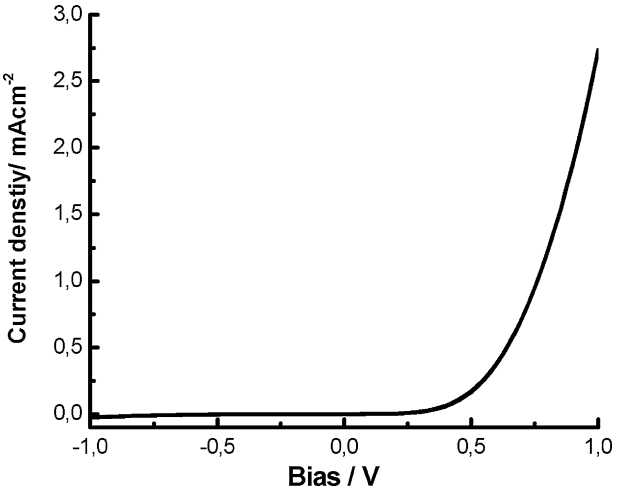

Fig. 10. *I–V* dark response of the TCO/d-TiO_2/nc-TiO_2/In_2Se_3/$CuInSe_2$/graphite cell. The complete cell was annealed in Se atmosphere at 400 °C for 30 min and etched in KCN solution during 1 min.

$CuInSe_2$, in agreement with a deposition mechanism proposed by other authors who have electrodeposited CISe on different substrates [20,21]. This is one of the reasons why most of the results are shown for CISe films electrodeposited during 60 min. Typical values for the thickness of CISe films electrodeposited at various times are shown in Table 1.

The data extracted from the transmission spectra recorded in CISe and In_2Se_3 films are converted into $(\alpha h\eta)^2$ versus $(h\eta)$ plots, in order to determine the band gap values (E_{gap}) of the films. The results for both films are shown in Fig. 9, leading to E_{gap} values of 1.04 and 1.66 eV, respectively. These values are in agreement with the literature for films electrodeposited on different substrates [6,22].

The quality of the TiO_2 films has been assessed by *I–V* measurements. The *I–V* response of d-TiO_2/graphite and d-TiO_2/nc-TiO_2/graphite Shottky barriers (0.07 cm^2 cell area) show almost perfect diode *I–V* behavior, excluding the presence of pinholes. When compared to results reported earlier [4], these samples have excellent rectification ratios, with values higher than 1000 for the d-TiO_2 and higher than 400 for the d-TiO_2/nc-TiO_2 bilayer (not shown).

Fig. 10 shows the *I–V* response of a TCO/d-TiO_2/nc-TiO_2/In_2Se_3/$CuInSe_2$/graphite cell. The curve shows a rectification ratio higher than 100. This indicates that the current due to internal shorts is moderate.

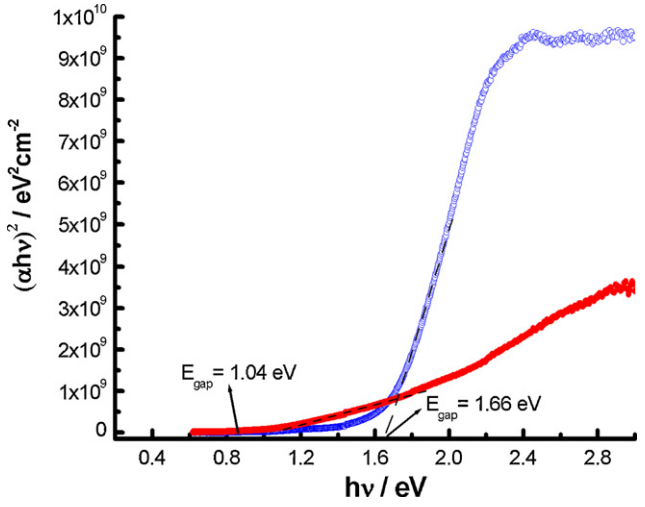

Fig. 9. E_{gap} determination for electrodeposited (○) In_2Se_3 and (●) $CuInSe_2$. The In_2Se_3 layer was prepared at −0.7 V (vs. SCE) during 20 min, while the $CuInSe_2$ was obtained at −0.8 V (vs. SCE) during 60 min. Both films were electrodeposited on d-TiO_2/nc-TiO_2.

4. Conclusions

In this work, TiO_2/In_2Se_3/$CuInSe_2$ heterojunctions have been prepared using electrodeposition and chemical spray pyrolysis. The morphology of both materials is very good, and also the physical and optical properties are in good agreement with those reported in the literature. Electrodeposition of a duplex layer of semiconductor compounds, each from a single bath and on top of a nanostructured material as substrate proved to be successful. Therefore, the quality of the materials seems promising for application in solar cells devices. In the case of the electrodeposited CISe film, annealing in selenium atmosphere and etching in KCN solution are essential to obtain a crystalline material and to remove secondary phases that are detrimental for the electronic properties of the film, respectively.

Raman spectroscopy proves to be a powerful technique to identify secondary phases on the films and for validation of the electrodeposition process as well.

The current–potential curves in the dark show a very good diode behavior. Present investigations focus on the photoconductivity and photovoltaic properties of these devices. Preliminary experiments indicate that although photoconductivity is clearly present, photovoltaic energy conversion is almost completely absent. This may indicate that the conduction bands of TiO_2 and $CuInSe_2$ are not properly aligned. In a future publication we plan to elaborate on this important issue.

Acknowledgements

The authors acknowledge the financial support received from the National Research Council of Argentina (CONICET), Agencia Nacional de Promoción Científica y Tecnológica (PICT 22-21440/04), Universidad Nacional de Mar del Plata, Argentina and SenterNovem, The Netherlands.

References

[1] B. O'Regan, M. Grätzel, Nature 353 (1991) 737.
[2] M. Nanu, J. Schoonman, A. Goossens, Nano Lett. 5 (2005) 1716.
[3] D. Lincot, J.F. Guillemoles, S. Taunier, D. Guimard, J. Sicx-Kurdi, A. Chaumont, O. Roussel, O. Ramdani, C. Hubert, J.P. Fauvarque, N. Bodereau, L. Parissi, P. Panheleux, P. Fanouillere, N. Naghavi, P.P. Grand, M. Benfarah, P. Mogensen, O. Kerrec, Sol. Energy 77 (2004) 725.
[4] M. Valdes, M.A. Frontini, M. Vazquez, A. Goossens, Appl. Surf. Sci. 254 (2007) 303.
[5] M.K. Nazeeruddin, A. Kay, I. Rodicio, R. Humphry-Baker, E. Müller, P. Liska, N. Vlachopoulos, M. Grätzel, J. Am. Chem. Soc. 115 (1993) 6382.
[6] S. Massaccesi, S. Sanchez, J. Vedel, J. Electroanal. Chem. 412 (1996) 95.
[7] B. Celustka, D. Bidjin, S. Porovic, Phys. Stat. Sol. (A): Appl. Res. 6 (1971) 699.
[8] R.C. West, M.J. Astle, W.H. Beyer (Eds.), CRC Handbook of Chemistry and Physics, 64th ed., CRC Press Inc., Boca Raton, Florida, 1983.
[9] M. Kemell, M. Ritala, M. Leskela, J. Mater. Chem. 11 (2001) 668.
[10] PDF Files No. 77-0452 (SnO_2), 23-0294(In_2Se_3), 40-1487($CuInSe_2$), 76-1865(Se_8), 26-0556(CuSe). JCPDS-ICDD (1998).
[11] A. Kampmann, A. Abken, G. Leimkuhler, J. Rechid, V. Sittinger, T. Wietler, R. Reineke-Koch, Prog. Photovolt.: Res. Appl. 7 (1999) 129.
[12] J. Weszka, P. Daniel, A. Burian, A.M. Burian, A.T. Nguyen, J. Non-Cryst. Sol. 265 (2000) 98.
[13] O. Volobujeva, J. Kois, R. Traksmaa, K. Muska, S. Bereznev, M. Grossberg, E. Mellikov, Thin Solid Films 516 (2008) 7105.
[14] C. Guillen, M.A. Martinez, J. Herrero, Vacuum 58 (2000) 594.
[15] Y. Sudo, S. Endo, T. Irie, Jpn. J. Appl. Phys. 32 (1993) 1562.
[16] J.F. Guillemoles, P. Cowache, A. Lusson, K. Fezzaa, F. Boisivon, J. Vedel, D. Lincot, J. Appl. Phys. 79 (1996) 7293.
[17] J.F. Guillemoles, A. Lusson, P. Cowache, S. Massaccesi, J. Vedel, D. Lincot, Adv. Mater. 6 (1994) 376.
[18] J.H. Park, I.S. Yang, H.Y. Cho, Appl. Phys. A: Sol. Surf. 58 (1994) 125.
[19] V. Izquierdo-Roca, A. Pérez-Rodríguez, A. Romano-Rodríguez, J.R. Morante, J. Álvarez-García, L. Calvo-Barrio, V. Bermudez, P.P. Grand, O. Ramdani, L. Parissi, O. Kerrec, J. Appl. Phys. 101 (2007) 103517-1.
[20] M. Kemell, M. Ritala, H. Saloniemi, M. Leskela, T. Sajavaara, E. Rauhala, J. Electrochem. Soc. 147 (2000) 1080.
[21] L. Thouin, S. Massaccesi, S. Sanchez, J. Vedel, J. Electroanal. Chem. 374 (1994) 81.
[22] R.P. Raffaelle, H. Forsell, T. Potdevin, R. Friedfeld, J.G. Mantovani, S.G. Bailey, S.M. Hubbard, E.M. Gordon, A.F. Hepp, Sol. Energy Mat. Sol. Cells 57 (1999) 167.